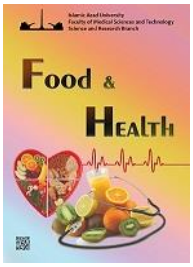

Food & Health Journal
Journal homepage: fh.srbiau.ac.ir

Investigating the structure and physicochemical properties of mucilage extracted from Malva flower

Amir Hossein Elhami Rad [1*], Atefeh Ghorbani [1], Leila Nateghi [2], Mohammad Hossein Haddad Khodaparast [3], Fatemeh Zarei [4]

[1] Department of Food Science and Technology, Sabzevar Branch, Islamic Azad University, Sabzevar, Iran
[2] Department of Food Science and Technology, Faculty of Agriculture, Varamin-Pishva Branch, Islamic Azad University, Varamin, Iran
[3] Department of Food Science and Technology, Ferdowsi University of Mashhad, Mashhad, Iran
[4] Food and Drug Administration, Tehran, Iran, Iran

ARTICLE INFO

Original Article

Article history:
Received 19 September 2021
Revised 02 April 2022
Accepted 23 April 2022
Available online 20 June 2022

Keywords:
Malva flower
Chemical structure
Mucilage
Hydrocolloids

ABSTRACT

In this study, the structure and physicochemical properties of mucilage extracted from Malva flowers were investigated. The mucilage suspension contains large particles with low polydispersity showing low stability due to low zeta potential. The morphology of particles indicates polyhedral monodisperse particles. The predominantly present element is potassium and the most important functional group by FTIR is carboxylate at the wavelength of 1623cm-1 and 1407 cm-1, pyranose vibratory ring at 1256cm-1, and 1062cm-1, and Beta configuration at 780 cm-1 and 618 cm-1. Results of NMR also suggested the presence of sugars in the mucilage. Its low enthalpy (193.27J/g) is due to the presence of ordered granules. Also, a high glass transfer temperature (95.4°C) indicates a high crystallization rate thus a stable structure and heat–resistant granules.

1. Introduction

Hydrocolloids are among additives widely used in the food industry in order to improve the quality of foods. Hydrocolloids are derived from various sources playing different roles including thickening, stabilizing, gelling and texture improvement. Although they are not true emulsifiers, they may be investigated as stabilizers because they extend the stability period of food systems. Plant–originated hydrocolloids are more acceptable than animal–derived ones by consumers (1). Mucilage is a common component among the plants which may be extracted from soft seeds or stems, e.g. mucilage of okra, psyllium, yellow mustard, and linseed (2). Malva is an annual, biennial, or hardly perennial plant belonging to the Malvaceae family. It originated in middle Asia and now is grown nearly all over the world including Iran. Malva flowers contain anthocyanins and mucilage and all parts of this plant especially its flower has healing effects on the respiratory system resulting from its high mucilage content (3). Malva is rich in A, B, and C vitamins and is effective in mitigating cold symptoms, especially coughing as well as respiratory, urinary ducts and digestive inflammation, and skin pimples. The results of some studies on the antimicrobial properties of Malva suggest that it has antibacterial, antifungal, and antiviral activity against human pathogens (4). Ameri et al., (5) investigated the properties of the new Malva leaf's gum. According to shear thinning behavior, Malva gum can be used in the food industry. Extracted gum showed a higher sensitivity to the temperature at the higher levels of gum concentration and the power law model was selected as the best model to assess the effect of gum concentration on the viscosity. Given that little information is available on the structure and physicochemical properties of Mucilage extracted from Malva Flower therefore the objective of this study was to investigate the chemical structure and physicochemical properties of mucilage extracted from malva

*Corresponding author: Department of Food Science and Technology, Sabzevar Branch, Islamic Azad University, Sabzevar, Iran.

E-mail address: ah.elhami@gmail.com (Amir Hossein Elhami rad).

flower allowing the application of vegetable hydrocolloids in different industries.

2. Materials and methods

2.1. Materials

Malva flowers were purchased from a local market in Tehran, Iran. The debris was separated from the flowers and then packed in hermetically sealed plastic bags and kept in a cool and dry place until extraction.

2.2. Extraction of Malva flower mucilage

To extract Malva flower mucilage a slightly modified method by Farahnaky et al., (6) was used. Malva flowers were ground and hydrated (seed powder: water, 1:50 w/v at room temperature for all night) . The mixture was centrifuged with (Rotofix 32 A, Germany) at 4000 rpm for 20 min at 25 °C to separate the mucilage. The gum solution was then separated, dried at 50 °C, ground, and then packed in hermetically sealed plastic bags and kept in a cool and dry place for later experiments. By rotation of these sharp blades, a hetero genus mixture of flower powder and mucilage was obtained. Then the mixture was centrifuged at 4000 rpm for 20 min at 25°C to separate the mucilage. The mucilage solution then was separated, dried at 50°C, ground, and placed in a dry and cool place for later experiments.

2.3. Zeta-potential, conductivity, and particle size

The zeta potential of 1g/L solutions was measured using the Malvern Zetasizer Nano series (Malvern Instrument, Worcestershire, UK) across the disposable, folded capillary cell (DTS 1060) at 25°C. The pH of the solutions ranged from 6.29 to 6.69. The conductivity of the samples and the particle size analysis were also measured. The conductivity and particle size of samples were also measured. A differential scanning calorimeter (INNUO DSC-500B, China) was used for DSC analysis of mallow seed mucilage. 5 mg sample was placed into a platinum cup and sealed. The temperature ranged from 20-300 °C under a nitrogen atmosphere with a heating rate being 10°C /min (7).

2.4. Determination of viscosity

The viscosity of 50 g/L solutions was measured by the use of a rheometer (Anton PAAR, MCR300, CC27, Austria). The effect of shear rate on the apparent viscosity of hydrocolloid solution at 0.1-1000 s^{-1} was investigated.

2.5. Differential scanning calorimetry (DSC)

DSC analysis for Malva flower mucilage was performed using a differential scanning calorimeter (INNUO DSC-500B, China). Accurately weighed (5mg) samples were placed into platinum cups and sealed. The temperature range was from 20°C to 300°C under nitrogen atmosphere at a heating rate of 10°C/min (7).

2.6. Scanning electron microscopy (SEM) and energy dispersive X-ray spectroscopy (EDS)

Scanning electron microscope (SEM) (TESCAN Vega-3 SBU model, Czech Republic) with an acceleration voltage of 5.0 kV was used. The samples were mounted on an aluminum stub with double-sided adhesive tape. The tape was attached to the stub and the sample powder was scattered carefully over its surface. The stub with the sample was then coated with a thin layer of gold to make the sample conductive. The specimen was subjected to SEM analysis (8). Quantitative elemental analysis and distribution of the elements (by X-ray mapping) in the Si/C composite were examined using the energy dispersive X-ray spectroscopy (EDS) analyzer attached with the SEM.

2.7. Fourier transforms infrared (FT-IR) analysis

FTIR spectra observed for the mucilage were recorded on a FT-IR spectrometer (Perkin Elmer spectrum 400, USA). The dry powder was mixed with KBr and pressed to form pellets under mechanical pressure. The FT-IR spectra were obtained at 4000 and 400/cm (9).

2.8. Nuclear magnetic resonance (NMR)

NMR spectra of 1H and 13C of mucilage were recorded in an NMR (250MHz) spectrometer (Bruker Avance model, Germany). The test mucoadhesive agent (100mg) was dissolved in D_2O and chemical variations were reported in ppm against an internal standard TSP (3-trimethylsilylpropionic-2,2,3,3,-d4 acid, sodium salt, 98% D) for 1H NMR and 1,4-dioxane (d 66.67 ppm) for 13C spectra. Proton NMR spectra were obtained at a base frequency of 250MHz, with 16 transitions and a delay time of 1.5 s and for 13C, the base frequency was 100MHz, with 3000 scans and a delay time of 2 s (10).

3. Results and discussion

3.1. Zeta-potential, conductivity, and particle size

In a colloid system, the potential difference between the stationary ionic layer (stern layer) and mobile layer (diffusion layer) in the ion atmosphere surrounding the charged particles is referred to as zeta potential. As shown in Fig. 1, 1g/L Malva flower mucilage solution showed a negative charge at pH 6.69 with a zeta potential of -17.5 mV. Zeta potential indeed is an indicator of the surface charge of particles and the potential stability of the emulsion system. If all particles in an emulsion have large negative or positive zeta potential they repulse each other, thereby promoting the system stability (11, 12). As general rule stability or instability of suspensions could be determined by zeta potential. The particles having zeta

potential of >30 mV or < -30 mV are stable. Therefore, Mallow flower mucilage suspension has little stability. Different factors including pH, ion strength, type and concentration of protein and polysaccharide macromolecules, their ratio, etc. affect the surface charge electrophoretic mobility and the zeta potential of the resulted complex (11). Electroactive biopolymers are a new class of natural compounds having conductivity as compared to synthetic polymers with high electrical conductivity. Recently, material scientific and technological potential regarding polymeric matrix in composites, pigments, and inhibitory and controlling nano-particles (oxygen, water, gas, and grease) are derived from polymers. Polymer electrolytes (PE) generally have ion conductivity in nature and they are electron conductive due to π- electron transfer. Of these two forms of electroactive polymer (EAP), the latter is referred to as intrinsic conducting polymers (ICP). In recent years, these polymers mostly belonging to electro-active polymers having great applicability potential have been paid much attention. Biopolymers have some functional properties in contrast to synthetic water-soluble and plant-derived gums. Natural polysaccharides also belong to EAP (13).

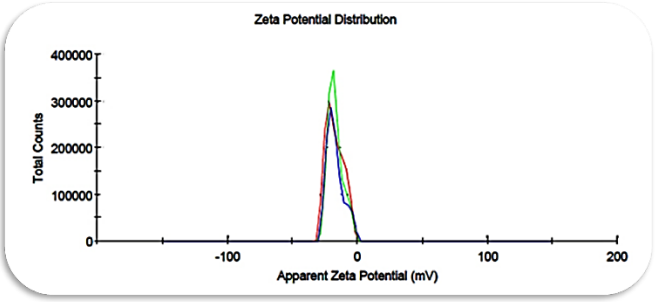

Fig.1. Zeta-potential in 1 g/L dispersion of Malva flower mucilage.

Malva flower mucilage solution (1g/L) has an electrical conductivity of 0.362 mS/cm. For practical purposes in the pharmaceutical-food industries, smaller particle sizes (at the nanoscale) are more desirable (11).

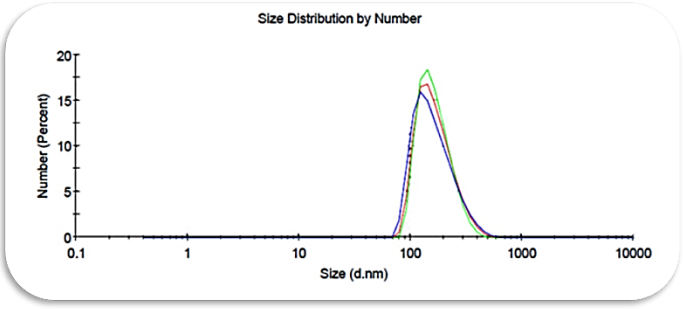

Fig. 2. Particles size in 1 g/L dispersion of Malva flower mucilage.

Particles size as average diameter Z (Z-average) in 1 g/L dispersion of Malva flower mucilage passed through a 0.45-micron filter is shown in Fig. 2. Average diameter of particles in the dispersion is 304.5 d.nm while polydispersity index (PDI) is 0.399. The results show large particles with low dispersity. Particle size and distribution in hydrocolloids are the most important parameters regarding hydration, solubility, and emulsion strength (14).

3.2. The viscosity of Malva flower mucilage solution

Fig. 3 shows the apparent viscosity dependence on the shear rate in 50 g/L mucilage solution of Malva flower. As can be seen, the apparent viscosity decreases with increasing cutting rate from 0.1 to 1000 s-1 from 0.04 to 0.009 pa.s, which indicates that the mucilage solution is plastic-like. The same behavior could be observed for most of the hydrocolloid solutions indicating the tendency of fluid toward Newtonian behavior and non- Newtonian behavior is indicated by the tendency towards zero (15).

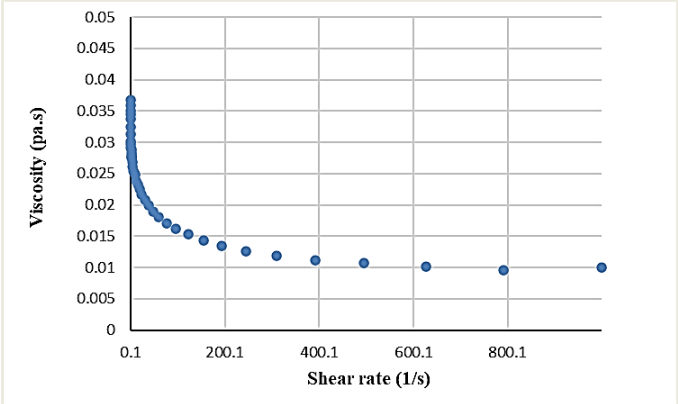

Fig.3. Apparent viscosity of 50g/L Malva flower mucilage solution at shear rate of 0.1-1000 1/s.

3.3. Differential scanning calorimetry (DSC)

DSC is used for the measurement of endothermal and exothermal changes with increasing temperature. It is widely used for the study of phase transitions of polymers because of its high sensitivity and accuracy (16). To do so the sample is heated under a certain controlled rate of gas flow (1:50 ml/min, 10°C/min) and then the difference in standard and sample (due to energy variations) is monitored by an appropriate sensor. The transfer is specified in the sample through energy absorption or release and is displayed as an endothermic or exothermic peak and/ or changes in baseline height in the cooling or heating curve. The area under the endothermic crystallization and exothermic melting curve is compared to the area for a standard sample (17). The thermogram for Malva flower mucilage is shown in Fig. 4. An endothermal peak indicating the melting process is seen at 135.2°C starting from 54.4°C to 202.3°C. The heat of fusion is seen at 193.27 J/g. Low enthalpy of this mucilage is due to the presence of ordered granules. Glass transition temperature (Tg) is observed at 95.4°C. Tg is defined in thermodynamic pseudo transition substances at which density, hardness and stiffness increase and elongation shows a significant decrease. It is also an intermediate temperature between the hard and melted states

of the materials. Above Tg secondary links of molecules are weaker relative to their thermal movements, because the polymer has found a lastic form and a certain elasticity and plastic deformation without breakage occurs (18). High Tg of Malva flower mucilage suggests its high rate of crystallization thus its stable structure and greater heat – resistance of granules. It is crucial to know Tg during production and storage when Tg is affected by moisture and other additives easily find a lastic state (16).

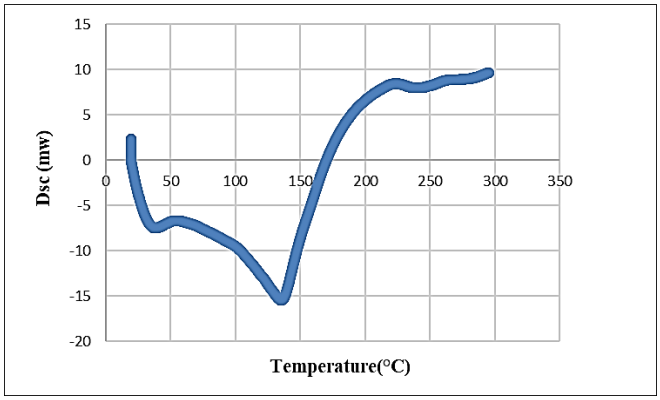

Fig. 4. Differential scanning calorimetry characterization of Malva flower mucilage Using DSC analyzer.

3.4. Scanning electron microscopy (SEM) and energy dispersive X-ray spectroscopy (EDS)

Fig. 5 exhibits the form and surface of the mucilage captured by scanning electron microscope (SEM). As shown in the figure it is in polyhedral form. Morphology and structure (topography) of mucilage surface may be affected by the procedure of extraction, purification, and/or preparation (19). SEM micrographs display monodisperse particles.

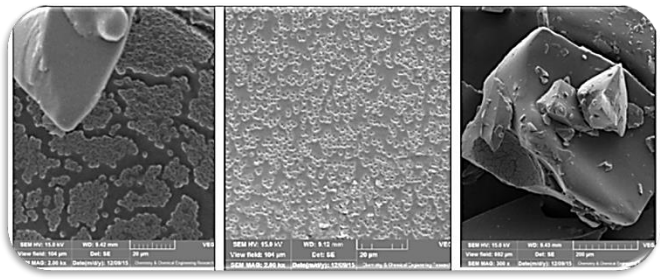

Fig. 5. SEM images of the powder particles of Malva flower mucilage.

These are spherically showing a compact and agglomerated structure. Some authors have suggested that static electrical effects and Van der Waals forces are the cause of this agglomerated structure. These particles consist of grains formed by sub-micron particles being connected by the compact structure (20). In this study, the elements were identified by the use of energy dispersive X-ray spectroscopy. The data obtained by this method are used for the quantity and quality identification of chemical compounds. The most predominant elements found in the Malva flower mucilage (Fig. 6) included potassium (25.03%), oxygen (23.61%), carbon (22.47%) sulphur (8.06%) nitrogen (6.73%) calcium (4.82%) phosphorus (4.12%) chlorine (2.16%) magnesium (1.63%) and sodium (1.32%).

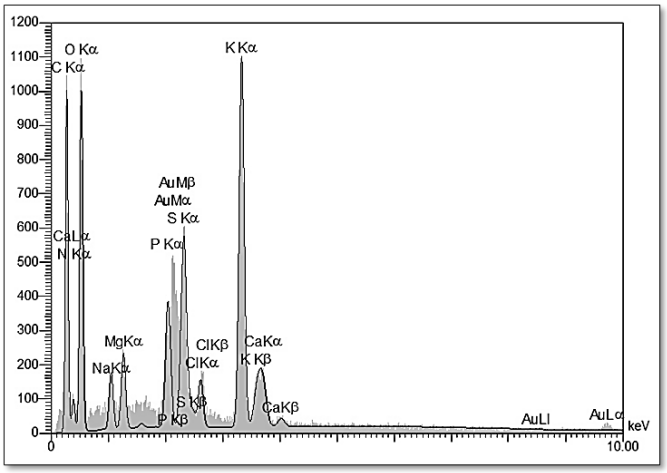

Fig. 6. Energy dispersive X-ray spectroscopy of the powder particles of Malva flower mucilage.

3.5. Fourier transform analysis (FTIR)

FTIR is widely used for describing the molecular polymer and materials structure. Characterization by FTIR is often due to the identification of functional groups and how they are connected to the polymer structure (21). FTIR reveals the peaks and band characteristics of Malva flower mucilage. FTIR results are shown in Fig. 7.

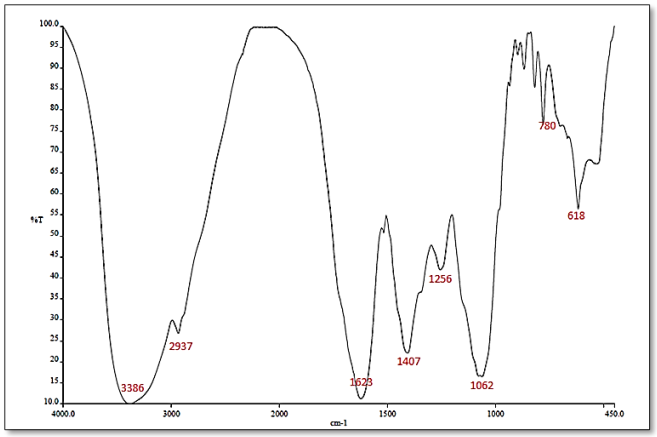

Fig. 7. FTIR spectral characterization of malva flower mucilage using Thermo Scientific FTIR spectrophotometer

The wide band at 3386 cm^{-1} is found for hydroxyl (-OH) groups. In general, the presence of a wide band at 3200-3500 cm^{-1} is fond for hydroxyl groups, whereas the band at 2937cm^{-1} is attributed to C-H asymmetrical vibrations. Natural sugars

typically contain acid sugar providing weak anion properties of the gum macromolecule (22). IR absorption of polysaccharides is characterized by a relatively strong peak at 1646 cm^{-1} (23). The absorbed bands at 1623 cm^{-1} and 1407 cm^{-1} are related to residual carboxylate groups of galacturonic acid. The area between 1500 cm^{-1} and 1800 cm^{-1} is used for the identification of carboxylic groups (24). Wave numbers between 800 cm^{-1} and 1200 cm^{-1} indicate the fingerprint area for carbohydrates (25). For peaks observed at 1062 cm^{-1} and 1256 cm^{-1}, the bands between 1000-1300 cm^{-1} are related to the vibratory ring of pyranose, while the absorbed signal at 618 cm^{-1} and 780 cm^{-1} is a Characteristic beta configuration in sugar sub-units.

3.6. Nuclear magnetic resonance (NMR)

Type, position, and area of H-NMR peaks are given in Table 1 and H-NMR peaks for the suggested compounds in the mucilage structure are shown in Fig. 8. As shown, chemical shift indicates the position of a certain proton, and peak height represents the area, i.e., the amount of that certain proton in the compound.

Table 1. Type, position and area of H-NMR peaks.

Peak height (Integral)	2.561	1.511	43.523	-
Chemical shift (ppm)	1.694-1.747[a]	2.957-2.985[b]	3.248-4.943[c]	6.263
Glucuronic acid (Gu)	-	-	+	-
Galacturonic acid (Ga)	-	-	+	-
Galactose (G)	-	-	+	-
Rhamnose (Ra)	+	-	+	-
Arabinogalactan (Ar)	-	-	+	-

[a,b]: Hydrogen of methyl ($-CH_3$) group in structures.
[c]: Hydrogen bonded carbon ((II) type) (-C-H-) and hydrogen bonded to oxygen in hydroxyl group (-O-H-) and/or carboxylic acid (-COOH) in structures.

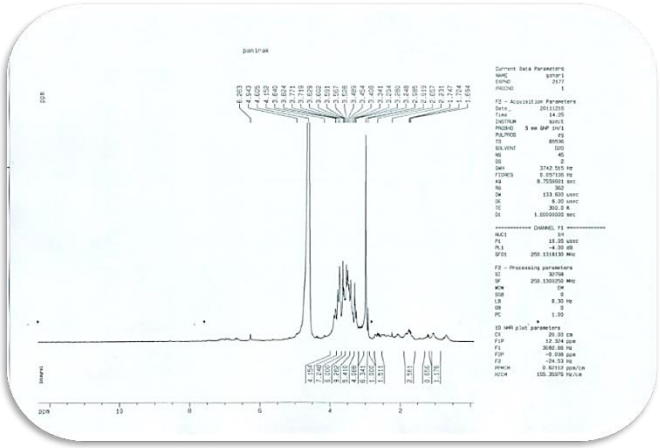

Fig. 8. H-NMR spectral characterization of Malva flower mucilage using Bruker Avance 250 NMR spectrophotometer.

The greater the integral value or peak area, the higher the amount of that proton. The peak related to first type methyl (-CH3) is visible which is present in rhamnose structure (1.69-1.74 ppm). Due to the overlapping effect of peaks at 3-4 ppm, the peaks observed for secondary carbon–bound protons (-C-H) and an alcoholic hydroxyl group (-OH) as well as carboxyl (-COOH) are coalescence and appeared at 3.24-4.9 ppm showing a large area and attributed to all protons (-C-H), (-OH) and (-COOH) in all compounds. C-NMR peaks for the suggested compounds in the mucilage structure are shown in Fig. 9 and the type and position of C-NMR peaks indicate in Table 2. C-13 in all compounds suggests the above compounds given the observed peaks. The peaks that appeared at 20 ppm suggest primary carbon, methyl carbon (-CH3), according to the structure rhamnosus, being found only in this class. The peaks observed within the 66-72 ppm area are related to secondary carbon where the hydroxyl group is bound to it being referred to as alcoholic or acid carbon in different configurations. This type of carbon is present in the structure of all compounds being appeared in the observed spectrum. The peak related to aldehyde carbon in the structure of the acid carboxylic (-C=0) functional group appeared within 173-182 ppm.

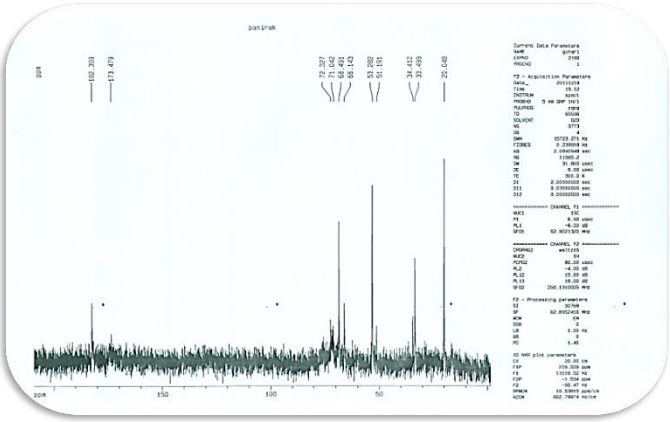

Fig. 9. C NMR spectral characterization of malva flower mucilage using Bruker Avance 250 NMR spectrophotometer

Table 2. Type and position of C-NMR peaks.

Chemical shift (ppm)	20.047[a]	33.49-34.41[b]	51.19-53.28[c]	66.14-68.49[d]	71.04-72.32[e]	173.47-182.39[f]
Glucuronic acid (Gu)	-	-	-	-	+	+
Galacturonic acid (Ga)	-	-	-	+	+	+
Galactose (G)	-	-	-	+	+	+
Rhamnose (Ra)	+	-	-	+	+	+
Arabinogalactan (Ar)	-	-	-	+	+	-

[a,b,c]: Carbon of methyl ($-CH_3$) and reveal (-C) of methyl in structure
[d,e,f]: Carbon ((II) type) bonded hydroxyl group in aliphatic chain (-CHOH-).

4. Conclusion

This study provides useful information on Malva flower mucilage as the physicochemical and structural properties of this hydrocolloid allow its application in cosmetics and pharmaceutical industries in addition to the food industry. Mucilage suspension has large particles with low dispersity showing weak stability due to low zeta potential. It may be

used for the stabilization of negatively charged colloid systems or sedimentation of positively charged systems due to its negative charge. Malva flower mucilage solution shows a non – Newtonian shear – thinning (pseudoplastic) behavior. Its low enthalpy (193.27 J/g) is due to the presence of ordered granules. Also, its high Tg (95.4°C) indicates its high crystallinity thus structural stability and heat–resistances of granules. The morphology suggests spherical polyhedral monodisperse particles. The most predominant element is potassium showing functional properties. The most important functional groups identified by FTIR are carboxylate at 1407 cm^{-1} and 1623 cm^{-1}, vibratory ring of pyranose at 1062 cm^{-1} and 1256 $cm^{-1,}$ and beta configuration at 618 $cm^{-1}$and 780 cm^{-1}. The results of NMR suggest the presence of rhamnose, galactose, arabinogalactan, and acid sugars glucuronic and galacturonic acids in the structure of mucilage.

References

1. Koocheki A, Taherian AR, Razavi SM, Bostan A. Response surface methodology for optimization of extraction yield, viscosity, hue and emulsion stability of mucilage extracted from Lepidium perfoliatum seeds. *Food Hydrocolloids*. 2009;23(8):2369-79.
2. Izydorczyk M, Cui SW, Wang Q. Polysaccharide gums: structures, functional properties, and applications. Food carbohydrates: Chemistry, physical properties, and applications. 2005;293:299.
3. Wichtl M. Herbal drugs and phytopharmaceuticals (translated from the German by Bisset, NG). CRC press scientific publishers; 1994.
4. Shale T, Stirk W, Van Staden J. Variation in antibacterial and anti-inflammatory activity of different growth forms of Malva parviflora and evidence for synergism of the anti-inflammatory compounds. *Journal of Ethnopharmacology*. 2005;96(1-2):325-30.
5. Ameri A, Heydarirad G, Mahdavi Jafari J, Ghobadi A, Rezaeizadeh H, Choopani R. Medicinal plants contain mucilage used in traditional Persian medicine (TPM). *Pharmaceutical Biology*. 2015;53(4):615-23.
6. Farahnaky A, Bakhshizadeh-Shirazi S, Mesbahi G, Majzoobi M, Rezvani E, Schleining G. Ultrasound-assisted isolation of mucilaginous hydrocolloids from Salvia macrosiphon seeds and studying their functional properties. *Innovative Food Science & Emerging Technologies*. 2013;20:182-90.
7. Stopić S, Ilić I, Uskoković D. Effect of Pd, Cu, and Ni additions on the kinetics of NiCl 2 reduction by hydrogen. *Metallurgical and Materials Transactions B*. 1997;28(6):1241-8.
8. Nep EI, Conway BR. Characterization of grewia gum, a potential pharmaceutical excipient. *Journal of Excipients and Food Chemicals*. 2010;1(1):30-40.
9. Sahoo N, Manchikanti P, Dey S. Herbal drugs: standards and regulation. *Fitoterapia*. 2010;81(6):462-71.
10. Hamcerencu M, Desbrieres J, Khoukh A, Popa M, Riess G. Synthesis and characterization of new unsaturated esters of gellan gum. *Carbohydrate Polymers*. 2008;71(1):92-100.
11. Khoshmanzar M, Ghanbarzadeh B, Hamishehkar H, Sowti M, REZAYI MR. Investigation of effective parameters on particle size, zeta potential and steady rheological properties of colloidal system based on carrageenan-caseinate nanoparticles. *The Journal of Research and Innovation in Food Science and Technology*. 2013;1(4):255-272.
12. McClements DJ. Protein-stabilized emulsions. *Current Opinion in Colloid & Interface Science*. 2004;9(5):305-13.
13. Pradhan SS, Sarkar A. Enhancement of electrical conductivity in the Gum Arabica complex. *Materials Science and Engineering: C*. 2009;29(6):1790-3.
14. Kaewmanee T, Bagnasco L, Benjakul S, Lanteri S, Morelli CF, Speranza G, et al. Characterisation of mucilages extracted from seven Italian cultivars of flax. *Food Chemistry*. 2014;148:60-9.
15. Abbasi S. Handbook of Elementary Rheology. By Howard Barnes), 1st ed, Marz-e-Danesh Publication. 2008:211.
16. Singh AK, Selvam RP, Sivakumar T. Isolation, characterisation and formulation properties of a new plant gum obtained from mangifera indica. *International Journal of Pharmacy & Biomedical Research*. 2010;1(2):35-41.
17. Chariyachotilert C, Joshi S, Selke SE, Auras R. Assessment of the properties of poly (L-lactic acid) sheets produced with differing amounts of postconsumer recycled poly (L-lactic acid). *Journal of Plastic Film & Sheeting*. 2012;28(4):314-35.
18. Cervantes-Martínez C, Medina-Torres L, González-Laredo R, Calderas F, Sánchez-Olivares G, Herrera-Valencia E, et al. Study of spray drying of the Aloe vera mucilage (*Aloe vera barbadensis* Miller) as a function of its rheological properties. *LWT-Food Science and Technology*. 2014;55(2):426-35.
19. Qian J-Y, Chen W, Zhang W-M, Zhang H. Adulteration identification of some fungal polysaccharides with SEM, XRD, IR and optical rotation: A primary approach. *Carbohydrate Polymers*. 2009;78(3):620-5.
20. Walton D, Mumford C. Spray dried products—characterization of particle morphology. *Chemical Engineering Research and Design*. 1999;77(1):21-38.
21. Baxter A, Dillon M, Taylor KA, Roberts GA. Improved method for ir determination of the degree of N-acetylation of chitosan. *International Journal of Biological Macromolecules*. 1992;14(3):166-9.
22. Wang Q, Ellis PR, Ross-Murphy S. Dissolution kinetics of guar gum powders-II. Effects of concentration and molecular weight. *Carbohydrate Polymers*. 2003;53(1):75-83.
23. Bremer PJ, Geesey GG. An evaluation of biofilm development utilizing non-destructive attenuated total reflectance Fourier transform infrared spectroscopy. *Biofouling*. 1991;3(2):89-100.
24. Figueiró S, Góes JC, Moreira R, Sombra A. On the physico-chemical and dielectric properties of glutaraldehyde crosslinked galactomannan–collagen films. *Carbohydrate Polymers*. 2004;56(3):313-20.
25. Ma J, Lin Y, Chen X, Zhao B, Zhang J. Flow behavior, thixotropy and dynamical viscoelasticity of sodium alginate aqueous solutions. *Food Hydrocolloids*. 2014;38:119-28.